Kovove Mater. 59 2021 149–160
DOI: 10.4149/km_2021_3_149

Mechanical and microstructural properties of friction stir welded AA5083 and AA5754 aluminium alloys

F. Tolun

Department of Motor Vehicles and Transportation Technologies, Balıkesir Vocational High School, Balıkesir University, 10145, Turkey

Received 31 January 2021, received in revised form 4 April 2021, accepted 21 May 2021

Abstract

Friction stir welding is a solid-state welding method for joining materials having the same or different properties at temperatures below their melting points. Generally, the welding parameters affect the microstructural and mechanical properties of welded specimens. In this study, AA5083 and AA5754 aluminium alloys were joined by friction stir welding at different tool rotation speeds of 450, 700, and 900 rpm, feed rates of 40, 50, and 80 mm min^{-1}, and tilting angles of 0°, 1°, and 3° using a tapered stir pin. The effects of these welding parameters on the mechanical properties of the welded parts were examined by tensile and micro-hardness tests. Moreover, the welded joints were analysed using an optical microscope, scanning electron microscope, and energy dispersive X-ray spectroscopy. The results indicated that the specimen welded at 50 mm min^{-1} feed rate, 450 rpm tool rotation speed, and a 1° tilting angle exhibited the highest welding strength and elongation values.

K e y w o r d s: friction stir welding, aluminium alloys, microstructure, tensile strength, microhardness elongation

1. Introduction

Friction stir welding (FSW) was patented in 1991 by The Welding Institute located in England [1] and used for the first time in the joining of Al alloys. The advantages of FSW are the shortened time for the welding process, automation compatibility, high welding strength values, obtaining smooth weld surfaces, and no requirement of additional weld metal and protective gas [2–4]. Al alloys, Mg alloys, Ti alloys, bronze, brass, steel, Cu, composite, and polymer materials can be successfully joined by the FSW method [5–15].

Tongne et al. [16] studied the joining of AA6082 T6 aluminium alloys by FSW. They developed a finite element analysis based on the Coupled Eulerian-Lagrangian formulation to predict and quantify the effect of FSW process parameters on the formation and extent of the banded structures. They found out via a combination of experimental and numerical analyses that the formation of the banded structures is mainly related to the geometry of the pin, whereas the friction conditions have a much smaller effect. Durdevic et al. [17] welded AA5754 H111 aluminium sheets with a "T" connection by FSW using different parameters. Their result showed that in the heat-affected zone (HAZ), there were higher values of microhardness for the specimen P4.1, which welded at 27 mm min^{-1} welding speed, 950 rpm tool rotation speed, 1° tilting angle, 5.8 mm tool plunge depth, 4 radii of backing plates than microhardness of specimen P4.2 which welded at 27 mm min^{-1} feed rate, 950 rpm tool rotation speed, 1° tilting angle, 5.8 mm tool plunge depth, 4 radii of backing plates. But, the highest values of microhardness were in joint P4.2 (70 HV1). Kumar and Kumar [18] studied the effects of different tool rotation speeds on the mechanical properties of the welded specimens of AA6063, and AA5083 Al alloys joined by FSW. They determined that the highest tensile strength, highest microhardness values, and the lowest bending strength were exhibited by specimens joined under the conditions of a tool rotation speed

*Corresponding author: e-mail address: ftolun@balikesir.edu.tr

of 1000 rpm at a 40 mm min^{-1} feed rate. Kumar et al. [19] examined the mechanical properties of AA5083-H111, and AA6082-T6 aluminium alloys joined by FSW. The results indicated that the welding efficiencies of the specimens were higher when different Al alloys are joined than those when the same Al alloys are joined.

The post-weld mechanical properties of Al6061 and Al6063 joined by FSW were examined by Devanathan et al. [20]. They used different tool rotation speeds while keeping other parameters constant (65 rpm feed rate and 5 kN axial force). They observed that the highest tensile strength (60 MPa) was when the tool rotation speed was 1800 rpm. When the speed was higher and lower than that value, the tensile strength was decreased, because at lower tool rotation speed stirring of the material was poor and heat input was lower. At a higher tool rotation speed, the unnecessary release of stirred material on the top surface leads to macroscopic defects because of the excessive heat input. Results obtained from the microstructural investigation showed that at 1800 rpm tool rotation speed, the grains were fine, uniform in size and distributed evenly, which results in higher strength. Kalemba-Rec et al. [21] studied the effects of process parameters on the mechanical properties of welded specimens of 7075-T651 and 5083-H111 Al alloys joined by FSW. They demonstrated that the tool rotation speed and the location of the alloy significantly affected the formation of the weld, especially in the stirring zone (SZ). Ren et al. [22] joined Al 5754 alloy by FSW using a cover sheet. They stated that with FSW using a cover sheet, higher welding strength and better bonding without metal loss and errors were obtained compared to the traditional FSW process.

The effects of the feed rate on microstructure and mechanical properties of AA5754 Al alloys joined by FSW were determined by El Rayes et al. [23]. As the heat input was reduced at high feed rates, grain and subgrain sizes, as well as the extent of recovery in the SZ, were reduced. They also reported that the increasing feed rate also increased the fragmentation and homogenised the second-phase particles within the SZ matrix. For this reason, it reduces the values of ductility and strain hardening exponent of the joint.

Ahmed et al. [24] investigated the effect of welding parameters on the joined dissimilar aluminium alloys (AA5083/AA5754 and A5083/AA7020) with FSW. The results showed that sound joints were obtained at the low heat input FSW parameters while increasing the heat input resulted in tunnel defects. The sound joints in both groups of the dissimilar joints showed very high joint strength with efficiency up to 97 and 98 %.

The effect of FSW parameters on the grain structure evolution in the nugget zone through the thickness of the 10 mm thick AA5083/AA5754 weldments was investigated by Ahmed et al. [25]. Results showed that the heating effect of the pressure and rotation of the pin shoulder and the heat input parameter on the hardness value of the nugget zone were dominating, and the tensile specimens of the welded joint at a tool rotation speed of 400 rpm and feed rate of 60 mm min^{-1} possessed the highest strain hardening parameter ($n = 0.494$).

Ahmed et al. [26] studied microstructure and mechanical properties of dissimilar FSWed AA2024-T4/AA7075-T6 T-butt joints. Results showed significant grain refining in SZ of FSW welds is accompanied by dynamic recrystallisation compared with the as-received base metals. Energy-dispersive X-ray spectroscopy (EDX) analyses of the SZ of the T-joints show four types of precipitates: $Al_6(Mn,Fe,Cu)$, Al_2Cu, Al_2CuMg, and $Al_7Cu_2Fe(C)$.

In the present study, non-heat-treatable alloys of AA5083 and AA5754 are used, as these alloys exhibit a high corrosion resistance, especially against seawater and chemicals. Due to this feature, they are widely used alone or in combination in shipbuilding and construction, chemical, automotive industries, and in the construction of pressure vessels [27, 28].

When these alloys are joined by fusion welding methods, they develop cracks and porosity problems in welding seams similar to other Al alloys. In addition, after welding, there is an increase in hardness values and a corresponding decrease in strength values. These problems can be solved by the FSW method. In joints made by FSW, high strength values and a good weld profile are observed in the welded specimens [29–33]. Therefore, in the present study, the effects of welding parameters on the mechanical and microstructural properties of the welded AA5083 and AA5754 Al alloy specimens were studied using the FSW method.

2. Experimental procedure

2.1. Materials used in the experiment

In this study, AA5083 and AA5754 Al alloy plates with dimensions of 4 mm × 100 mm × 150 mm were used as the base material. The chemical compositions and mechanical properties of these alloys determined by Aydınlar Metal Industry and Trade Inc., Turkey are given in Tables 1, 2.

2.2. Tool used in the experiment

A tapered pin tool made of 1,333 high-speed steel and having a hardness of 62 HRC by using a heat treatment was used in the study. Its shoulder diameter was 15 mm, pin depth 3.87 mm, the outer diameter of the tapered pin 4 mm, and inner diameter 2 mm (Fig. 1a).

Table 1. Chemical composition of AA5083 and AA5754 aluminium alloys (wt.%)

Alloy element	Si	Fe	Mn	Mg	Cu	Ti	Cr	Zn
AA5083	0.112	0.318	0.535	4.783	0.073	0.012	0.062	0.128
AA5754	0.093	0.191	0.164	2.774	0.003	0.007	0.004	0.007

Table 2. Mechanical properties of AA5083 and AA5754 Al

	Tensile strength (MPa)	Yield strength (MPa)	Elongation (%)	Hardness HV
AA5083	237.41	159.5	17.06	75
AA5754	226.82	108.6	16.19	52

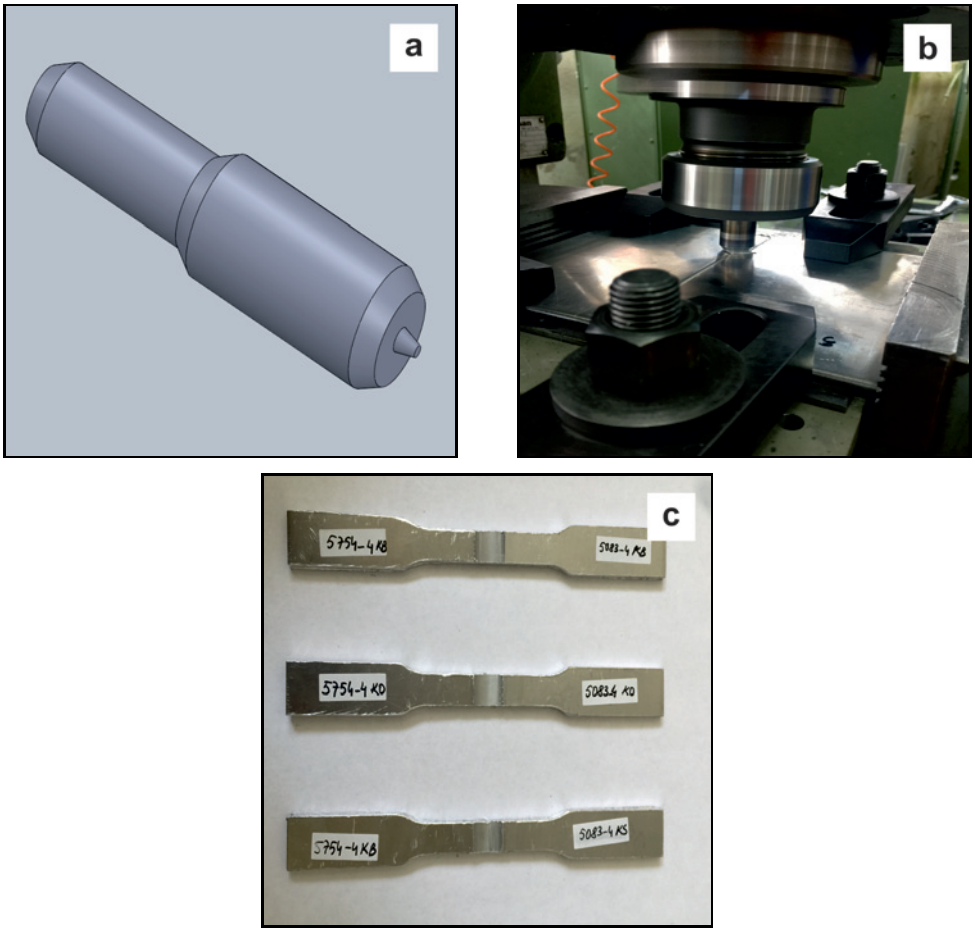

Fig. 1. Images of (a) tapered pin tool, (b) FSW operation in the Universal Milling Machine, and (c) tensile test specimens.

2.3. FSW experiment

AA5083 and AA5754 Al plates were joined with butt welding by the FSW method (Fig. 1b). The welding process was carried out in the Universal Milling Machine (Taksan FU 315 × 1250) at room temperature. Before welding, all surfaces of the test specimens were smoothened by milling. The welding surfaces were sanded by hand and then wiped with pure alcohol. The specimens prepared for welding were firmly fixed on the milling machine by a fishplate.

Welding operations were carried out with different parameters selected after preliminary experiments. In the joining process, the tool rotated in a clockwise direction, and the waiting time at the start of welding was taken as 60 s. In accordance with the literature, AA5083, a harder Al alloy than AA5754 was placed on the advancing side and AA5754 on the retreating side. The welding parameters of the experiments performed at different feed rates, different tool rotation speeds,

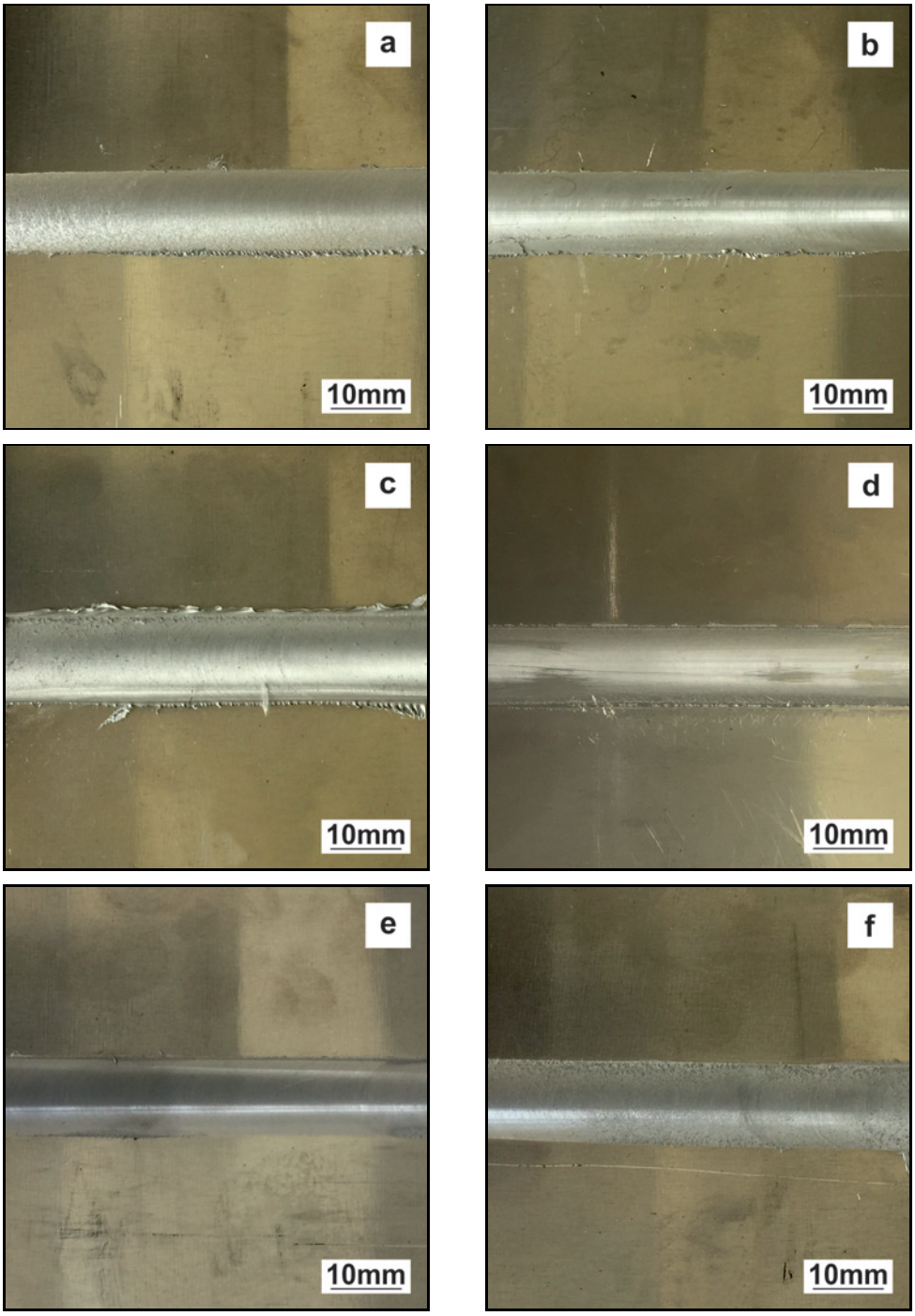

Fig. 2a–f. Surface images of (a) specimen 1, (b) specimen 2, (c) specimen 3, (d) specimen 4, (e) specimen 5, (f) specimen 6.

and different tilting angles are presented in Table 3. In the coding of the welding parameters, the values of the feed rate, tool rotation speed, and tilting angle were used as 40/450/0, respectively.

After the FSW process, tensile tests were performed on the specimens using the Zwick Roel tensile testing device. For each condition, three specimens were prepared with the welding seam in the middle and in accordance with the ASTM E08 M-04 standard [34]. The tensile specimens (Fig. 1c) were drawn perpendicular to the welding direction at a drawing speed of 2 mm min^{-1}, and the tensile strengths were measured.

The microstructural changes after the FSW process were examined using an optical microscope (OM; Nikon DS-Fi), the scanning electron microscope (SEM; JEOL JSM-6060) images of the welded specimens, and EDX analysis. For this, specimens were first inserted in the polyester mould for microscopic examinations and sanded with sandpaper 220-1200. Then,

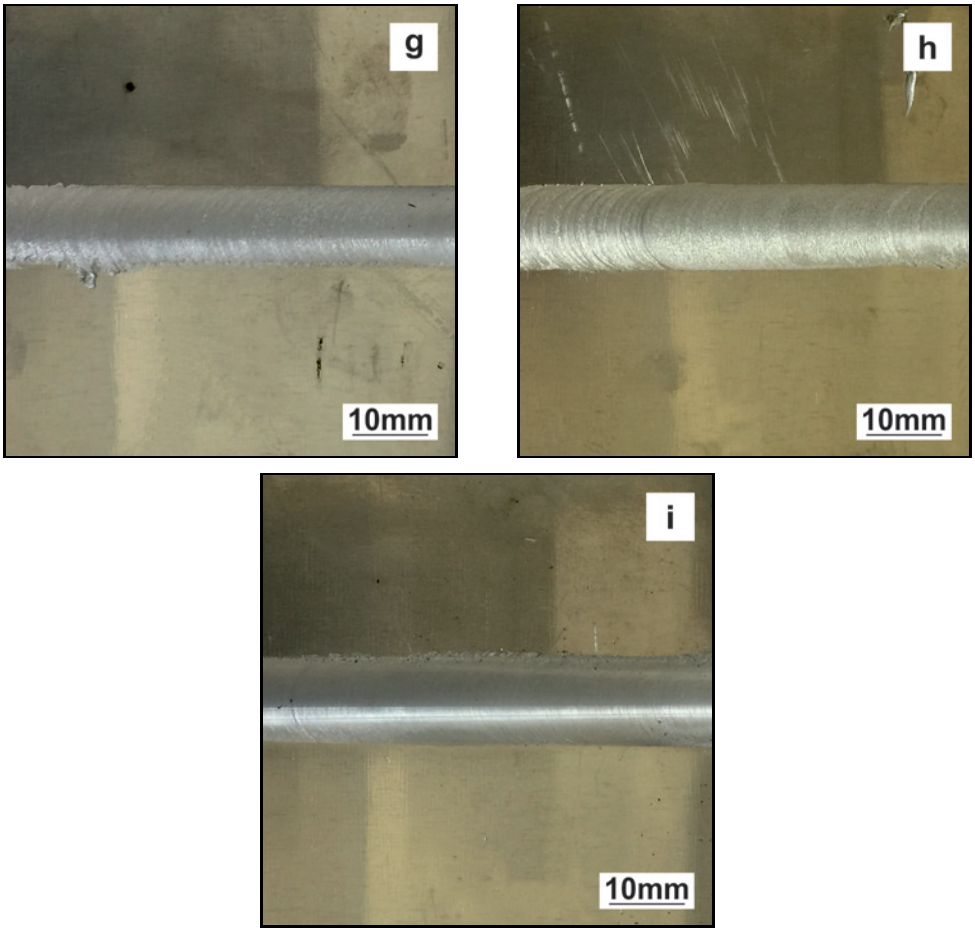

Fig. 2g–i. (g) specimen 7, (h) specimen 8, and (i) specimen 9.

Table 3. The detailed welding parameters used in this study

Treatment no.	1	2	3	4	5	6	7	8	9
Feed rate (mm min^{-1})	40	40	40	50	50	50	80	80	80
Tool rotation speed (rpm)	450	700	900	450	700	900	450	700	900
Tilting angle (°)	0	1	3	1	3	0	3	0	1

they were polished with 3 and 1 μm diamond paste and etched with Poulton reagent, which was obtained by mixing 50 ml Poulton solution, 25 ml concentrated HNO_3, and 40 ml chromic acid solution. Specimens were gold plated for SEM imaging.

The hardness values of the specimens were measured on the Vickers scale (HV0.1) using the Shimadzu HMV micro-hardness tester along a line perpendicular to the welding seam direction on the welding surface. The measurement load was 0.1 kg, and the waiting time before the measurement was 15 s.

3. Results and discussion

The results of the FSW welding of AA5083 and AA5754 aluminium alloys are given below. Figures 2a–i show the surface images of welded specimens. Figure 2a shows specimen 1(40/450/0), Fig. 2b shows specimen 2(40/700/1), Fig. 2c shows specimen 3(40/900/3), Fig. 2d shows specimen 4(50/450/1), Fig. 2e shows specimen 5(50/700/3), Fig. 2f shows the specimen 6(50/900/0), Fig. 2g shows the specimen 7(80/450/3), Fig. 2h shows the specimen 8(80/700/0), and Fig. 2i shows the specimen 9(80/900/1).

Figure 2 indicates that the welding seams of specimen 2, 3, 4, 5 were smooth and uniform, while those of specimen 1, 6, 7, 8 were rough. Therefore, the rough structure noticed in the welding seam of specimens 1, 6, 7, and 8 was thought to negatively affect the mechanical values of the weld [11, 35]. According to the tensile test results, microstructure analyses and

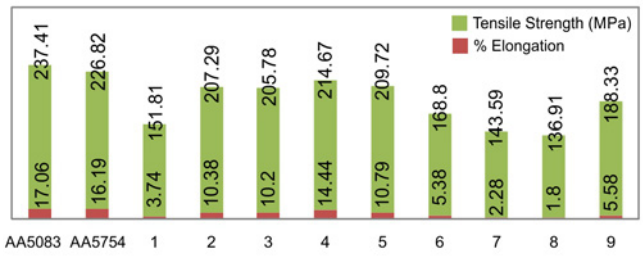

Fig. 3. Tensile strength and percentage elongation values of specimens.

microhardness tests were performed for specimen 4, for which the highest welding strength was detected, and specimen 8, for which the lowest welding strength was determined. Since the other specimens are among these two specimens in terms of welding strength, the microstructure analyses and microhardness tests were not performed.

The tensile test was performed to determine the welding strength values of the welded specimens (Fig. 3).

High temperatures and intense plastic deformations occur within the material from the FSW process, causing recrystallisation in the SZ. This causes the precipitates to dissolve and become rough around the SZ. It is known that the internal structure forms after the FSW process are divided into three different zones: dynamic recrystallisation SZ, thermo-mechanical affected zone (TMAZ), and HAZ. The weakest and least hardened area of the welding zone is the HAZ zone. During the welding process, the precipitate particles continue to grow in the HAZ and show excess ageing or coarsening, and the distance between the particles increases. Therefore, dislocations move easily in this area without encountering any obstacles, thereby reducing the strength. In the tensile tests carried out on specimens of AA5754 and AA5083 alloys, the rupture was always seen to occur in the HAZ and ductile fracture on the side of the AA5754 specimen. The cracks developed on the side of the AA5754 specimen owing to its slow tensile strength compared to that of AA5083; this is consistent with the literature [23, 26, 35, 36].

As different welding parameters affect the mechanical properties of welded specimens, the feed rate, tool rotation speed, and tilting angle parameters must be evaluated together [18, 20, 24].

The selection of the optimum welding parameters, which are feed rate, tool rotation speed and tilting angle, are important for a high strength welding process and to decrease welding defects and porosity.

Heat input is one of the important parameters for FSW. It plays a significant role in controlling the joints properties and quality. Tool rotation speed and feed rate control the heat input in the welding area during the FSW. Tool rotation speed and feed rate determine the amount of frictional heat generated, followed by plastic deformation and deformation heat. Therefore, it is important to choose the appropriate combination of them for a defect-free joint with a good metallurgical bond and mechanical properties. Tool rotation speed affects the intensity of plastic deformation occurring in the weld zone during the welding and through this affects material mixing. Feed rate controls the thermal cycle, residual stresses, and production rate. High tool rotation speed with the unnecessary release of stirred material on the top surface leads to macroscopic defects, such as poor surface (flash), voids, porosity, tunnelling, or wormhole formation, due to the extremely high heat input generated welding. Low tool rotation speed leads to a poor stirring of the material and low heat input. Increasing the feed rates led to decreasing heat input to the welding zone by lowering the time duration of tool-workpiece interaction at a given point of action. Reducing the feed rates led to increasing heat input to the welding zone. Moderate amounts of heat inputs are suitable for the plastic deformation, stirring, and material flow in FSW [24, 37, 38].

Studies also support that during the FSW process, welding operations performed by using tilting angle showed good mechanical properties [16, 17, 39]. The results of this study demonstrated that the tilting angle also has an important effect on the mechanical properties of the welded specimens. High strength values were observed in the welding processes when a 1° tilting angle was used. When it was increased to 3°, a decrease in the tensile strength values was observed. In particular, the lowest tensile strength values were obtained when the tool was kept vertical (tilting angle = 0°).

As seen in Table 2, the tensile strength and the elongation values of the AA5083 alloy were 237.41 MPa and 17.06 %, respectively. However, the corresponding values of AA5754 alloy were 226.82 MPa and 16.19 %, respectively. According to the tensile test results, specimen 4(50/450/1) showed the highest tensile strength value (214.67 MPa) and percentage of elongation value (14.44 %). The tensile strength of specimen 4 was 90.41 % and 94.64 % of that of AA5083 and AA5754, respectively. By maintaining the feed rate at 50 mm min^{-1}, increasing the tool rotation speed, and changing the tilting angle, the tensile strength and elongation values decreased. The tensile strength of specimen 5(50/700/3) decreased to 209.72 MPa, and the elongation decreased to 10.79 %. When the tool rotation speed was increased to 900 rpm, and the tilting angle was reduced to 0° while keeping the feed rate constant at 50 mm min^{-1}, the tensile strength of 168.8 MPa and elongation of 5.38 % were obtained from specimen 6(50/900/0). When the

feed rate was reduced to 40 from 50 mm min^{-1}, tensile strength and % elongation values decreased. The tensile strength value and elongation of specimen 2(40/700/1) were 207.29 MPa and 10.38 %, respectively. When the tilting angle was increased to 3°, and the tool rotation speed was increased to 900 rpm at a constant feed rate of 40 mm min^{-1}, the tensile strength value of specimen 3(40/900/3) decreased to 205.78 MPa and elongation decreased to 10.20 %. Furthermore, when the tilting angle was decreased to 0°, and the tool rotation speed was reduced to 450 rpm at a constant feed rate of 40 mm min^{-1}, the tensile strength of specimen 1(40/450/0) decreased to 151.81 MPa and the elongation to 3.74 %. Specimens joined at a feed rate of 80 mm min^{-1} showed lower tensile strength and elongation values. The tensile strength was determined as 188.33 MPa and elongation as 5.58 % for specimen 9(80/900/1). Thus, the high tool rotation speed of this specimen at a high feed rate also affected the tensile strength positively. Selecting low tool rotation speeds at high feed rates during welding reduced the tensile strength and elongation values. When the tilting angle was increased to 3°, and the tool rotation speed was reduced to 450 rpm at a constant feed rate of 80 mm min^{-1}, the tensile strength of specimen 7(80/450/3) was found to decrease to 143.59 MPa and elongation to 2.28 %.

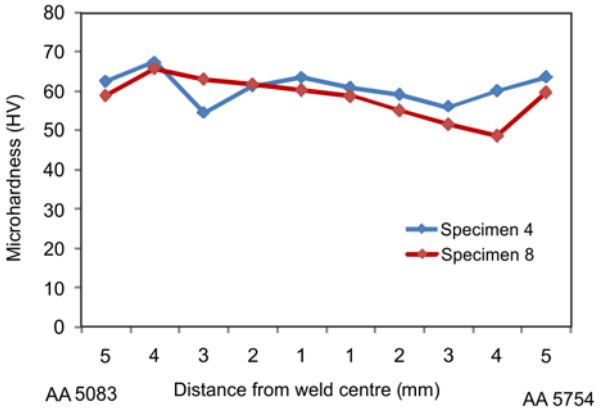

Fig. 4. Micro-hardness variation of specimens 4 and 8.

When the tilting angle was decreased to 0°, and the tool rotation speed was increased to 700 rpm at a con-

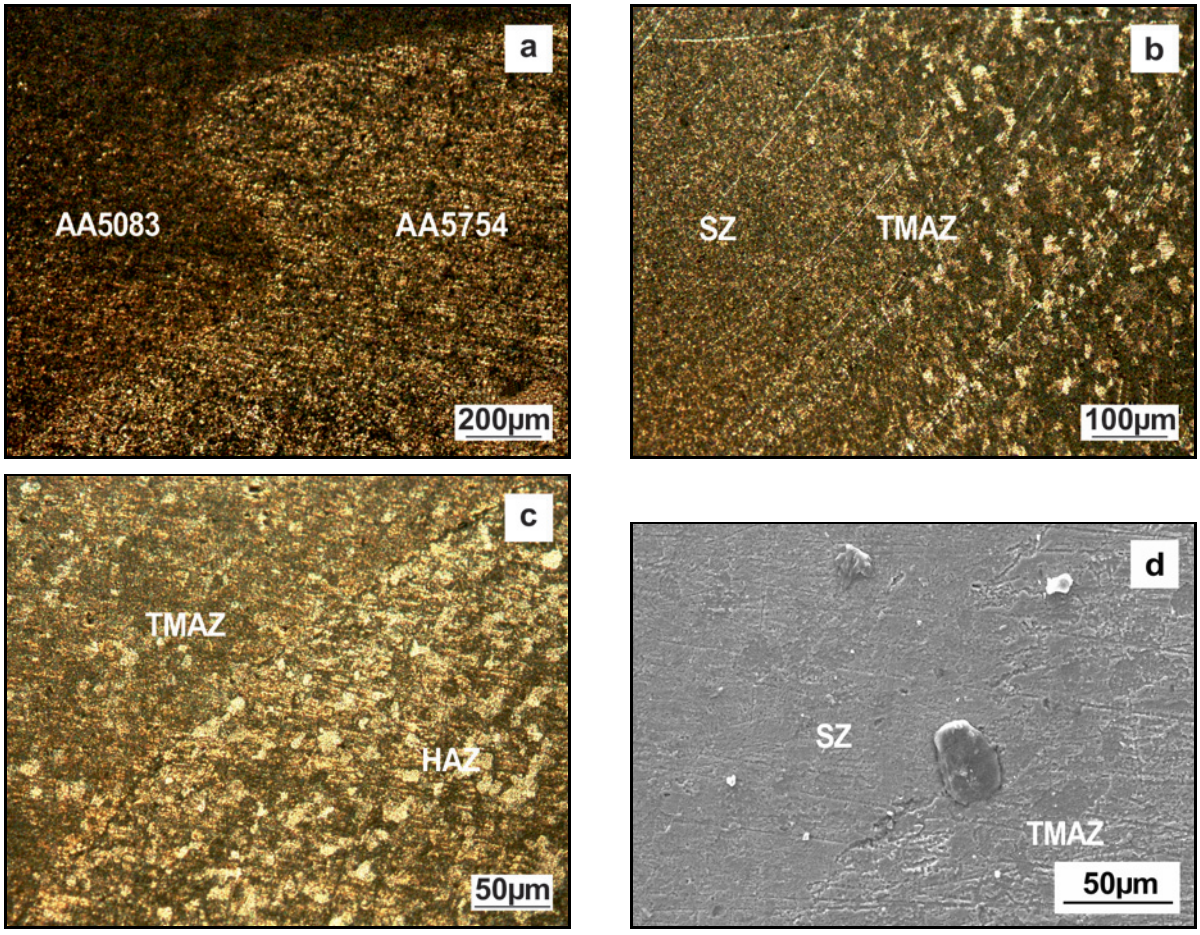

Fig. 5. OM and SEM images of (a) the welding zone, (b) SZ and TMAZ regions, (c) TMAZ and HAZ regions, and (d) defects in the welding zone of specimen 4.

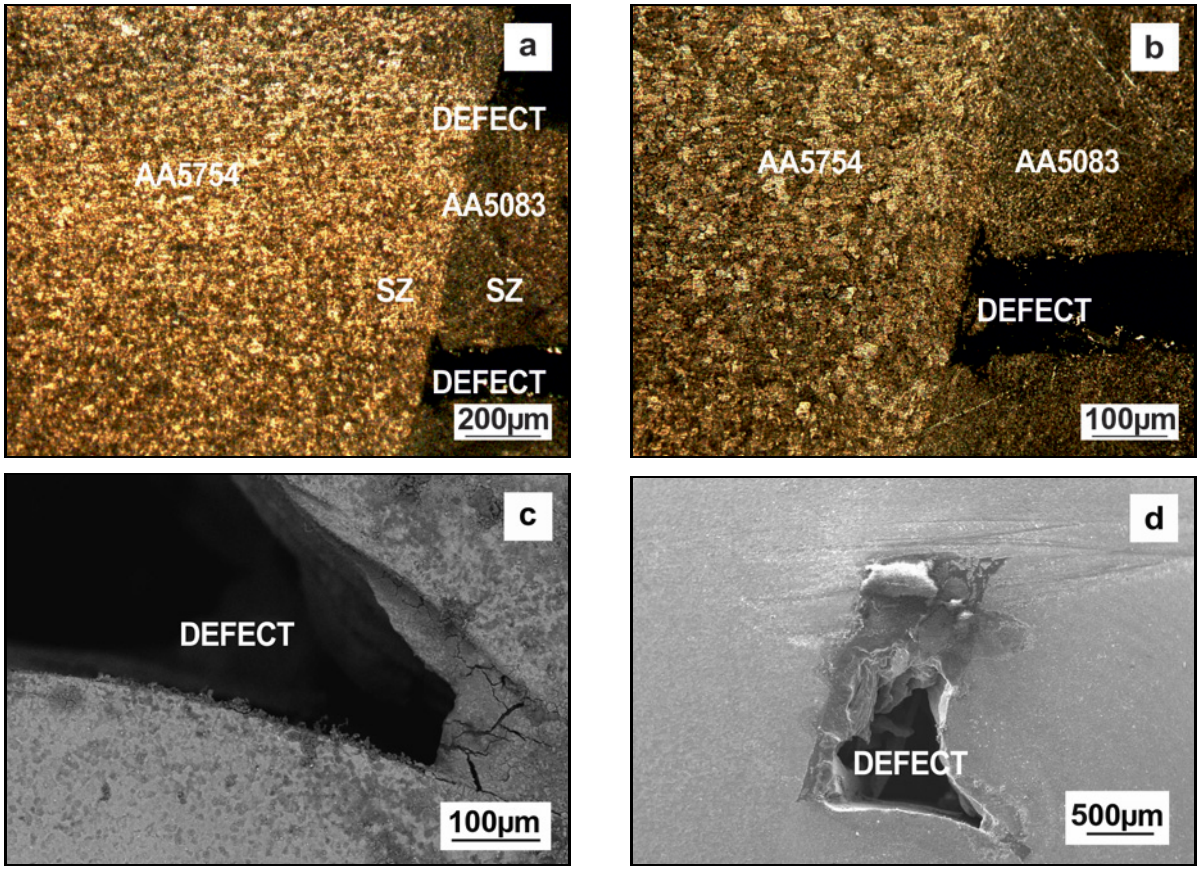

Fig. 6. OM and SEM images of (a) the welding zone, (b) SZ and TMAZ regions, and (c) and (d) defects in the welding zone of specimen 8.

stant feed rate of 80 mm min^{-1}, specimen 8(80/700/0) showed the lowest tensile strength and percentage elongation values. The tensile strength value and percentage elongation of specimen 8 were 136.91 MPa and 1.80 %, respectively. Its tensile strength was 57.66 % of AA5083's value and 60.36 % of AA5754's value. Due to the high feed rate, low tool rotation speed and lack of tilting angle, full stirring could not be achieved in the welding zone, and heat input was not sufficient for high strength joining. This led to the generation of welding defects in the welding seam. It is thought that these welding errors, which can also be observed in macro dimensions, were responsible for decreasing the welding strength. A linear relationship was observed between the elongation and tensile strength values, and thus, the elongation values decreased with the decrease in the tensile strength.

Welded specimens joined at a 50 mm min^{-1} feed rate and a 1° tilting angle showed the best mechanical properties in terms of the tensile strength and elongation values. Thus, these conditions were selected as the optimum welding parameters to obtain good mechanical properties.

Figure 4 shows the changes in the microhardness values of the welding zones of specimen 4 (highest tensile strength) and specimen 8 (lowest tensile strength). It shows that there are small changes in the hardness values in the welding zones of both specimens. This is explained by forming a welded structure with homogeneous distribution and properties close to those of the base metals.

In general, the microhardness profile in all welds was maximum in the SZ and decreased towards the base metal. The SZ was thinner than the grain size. Some changes in the hardness values may have been caused by the $Al_x(Fe,Mn)_ySi_z$, $Al_x(Fe,Mn)$, and Mg_xSi intermetallic phases that formed owing to the heat input in the welding zone during the FSW process of AA5XXX Al alloys [40, 41].

Figure 5a shows OM images of the welding zone of specimen 4 (highest welding strength), which demonstrate that AA5754 and AA5083 aluminium alloy materials stirred properly with each other in the welding zone. This figure also shows the fine-grained structure of the SZ having a homogeneous distribution where the stirring occurs via the stirring pin. Increasing the temperature and stirring effect of the pin increased the extrusion degree in the material, which became viscous. Therefore, a structure with grain shrinkage and hardening emerged in the SZ. The deformation and extrusion intensity generated during the FSW process, and caused

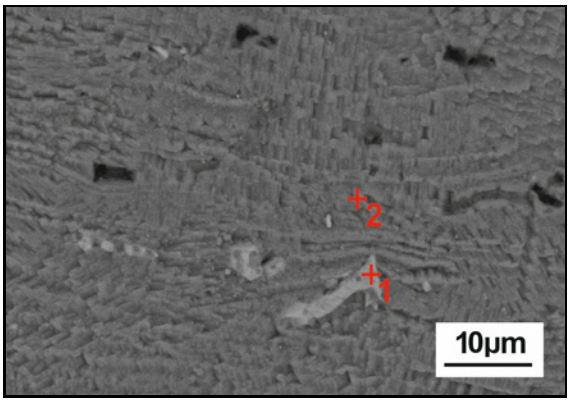

Fig. 7. Welding area of specimen 4.

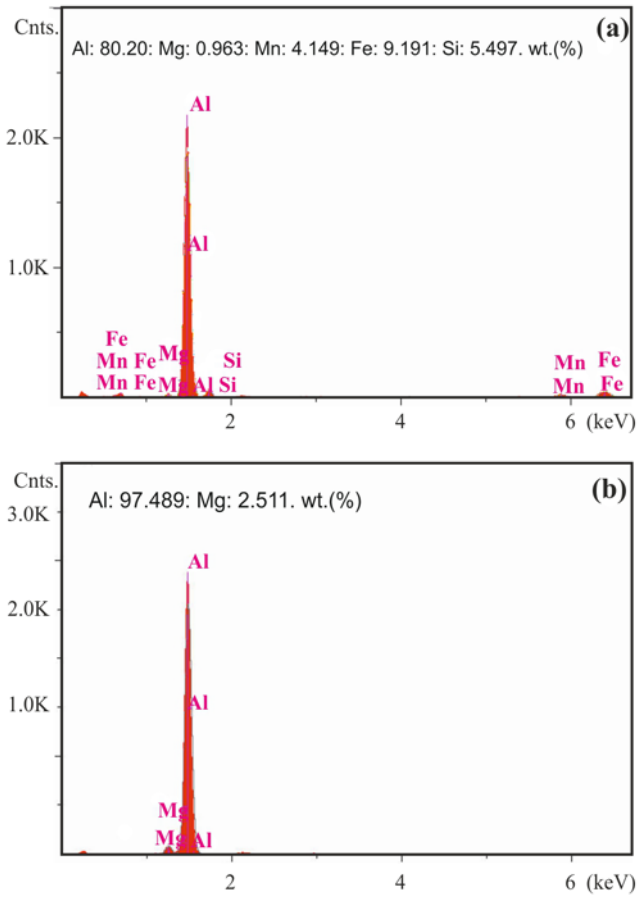

Fig. 8. EDX analysis number of (a) 1 and (b) 2 of SZ of specimen 4.

the grains to shrink in the SZ.

In Fig. 5b, the SZ and TMAZ regions can be clearly observed in the welding zone of specimen 4. In TMAZ, a bigger-sized coarse-grained structure stands out compared to the grain size in SZ. This can be attributed to the lower heat input to TMAZ and plastic deformation during the welding process compared to SZ. In Fig. 4c, HAZ is the weakest region of the welding zone [35, 40–42].

Figures 5c,d show SEM images of the welded zones of specimen 4, with fine-grained and coarse-grained structures in the SZ and TMAZ regions, respectively. The SEM images of specimen 4 show that intermetallic components occurred in the welded zone, which can be observed as white specks. SEM images and OM images show that specimen 4 has been successfully welded by FSW.

The OM images of the welding zone of specimen 8 (lowest welding strength) are presented in Figs. 6a,b; a fine-grained SZ and coarse-grained TMAZ can be observed. Gaps between the joints of AA5033 and AA5754 materials are noticeable in the welded zone, which represent undesirable welding defects in the joining process and also reduce the welding strength. These defects explain the reason for the decrease in tensile strength.

The SEM and OM images of specimen 8 indicate welding defects that are detected and cause a decrease in the welding strength of the specimen. Such defects are shown in Figs. 6c,d.

Figures 7 and 8 present the results of EDX analysis of specimen 4, which represent the welding area, analysis number 1, and analysis number 2 of the SZ, respectively. It is seen that $Al_x(Fe,Mn)_ySi_z$, $Al_x(Fe,Mn)$, and Mg_xSi intermetallic phases occur because of the heat input in the welding zone during the FSW process of AA5XXX Al alloys. Essentially, 5xxx series alloys are single-phase type alloys (e.g., Al_3Mg_2, $Al_6(Fe,Mn)$). Phases such as Al_6Mn, Al_3Fe, and Al(Fe,Mn,Si) are dispersed in the aluminium matrix as secondary phase particles, out of which Al_3Mg_2 is seen to occur at 450 ℃. This causes the Mg deficiency in the grain boundaries by structuring between the grains and the grain boundaries. The Al_6Mn phase is an intermetallic phase with a melting temperature of 705 ℃. The melting temperature of this phase is higher than the solidus temperature of the AA5754 alloy [35, 40, 41].

Analysis number 1 of the SZ region of specimen 4 (Fig. 8a) demonstrates that the densities of Si, Mn, Fe, Al, and Mg elements increased significantly.

Analysis number 2 of specimen 4 (Fig. 8b) shows that only Al and Mg elements were observed in the structure. Analysis number 2 of specimen 4 indicates that the Si, Mn, and Fe elements observed in the structure support the presence of Al_3Mg_2, $Al_6(Fe,Mn)$, Al_6Mn, Al_3Fe, and Al(Fe,Mn,Si) phases in the welding zone.

4. Conclusions

AA5083 and AA5754 Al alloy plates were welded

by the FSW method in this study. Specimen 4 exhibited the highest tensile strength and elongation values. The tensile strength of specimen 4 was 90.41 % and 94.64 % of that of AA5083 and AA5754, respectively. Specimen 8 had the lowest tensile strength and elongation value. Its tensile strength was 57.66 % and 60.36 % of the values corresponding to of AA5083 and AA5754, respectively. A linear relationship was observed between the percentage elongation and tensile strength values of the specimens.

Because of the high feed rate, low tool rotation speed, and no tilting angle, complete stirring in the welding zone was not achievable. This caused welding defects to develop in the form of gaps in the weld seam, which decreased the welding strength. Microstructure analyses also supported these findings. The defects and the form of gaps can be prevented by using optimum welding parameters.

Welding processes at a 50 mm min^{-1} feed rate gave the highest tensile strength and elongation values. When the feed rate was reduced to 40 mm min^{-1} or increased to 80 mm min^{-1}, the tensile strength and elongation values decreased. The effect of tool rotation speed on tensile strength and elongation values varied according to the selected feed rate and tilting angle.

High welding strength values were observed when welding was performed at a 1° tilting angle. When the tilting angle was increased to 3°, tensile strength values decreased. The lowest tensile strength values were obtained when the tool was kept vertical.

Finally, small changes in hardness values in the welding zone were also observed. The increasing hardness of $Al_x(Fe,Mn)_ySi_z$, $Al_x(Fe,Mn)$, and Mg_xSi intermetallic phases occurring because of heat input in the welding zone during the FSW process of AA5XXX Al alloys caused these changes in the hardness values. When EDX analysis of specimen 4 in SZ was examined, the density increase of Mg, Si, Mn, and Fe elements supported the presence of Al_3Mg_2, $Al_6(Fe,Mn)$, Al_6Mn, Al_3Fe, and Al(Fe,Mn,Si) phases in the welding zone. Phase analysis was not performed in this study. In further studies, the presence of these phases should be determined by phase analysis.

AA5754 and AA5083 Al alloys are widely used alone or in combination in the industry. The findings obtained from this study can be used in joining AA5754 and AA5083 Al alloys with the FSW method in practical applications.

Acknowledgements

The authors would like to thank Aydinlar Metal Industry and Trade Inc., Turkey, for providing the Al alloy sheets.

References

[1] M. Kumagai, Recent technological developments in welding of aluminium and its alloys, Welding International 17 (2003) 173–181. doi:10.1533/wint.2003.3074

[2] S. M. Bayazid, H. Farhangi, A. Ghahramani, Investigation of friction stir welding parameters of 6063-7075 aluminum alloys by Taguchi method, Procedia Material Science 17 (2015) 6–11. doi:10.1016/j.mspro.2015.11.007

[3] R. Ranjan, A. R. Khan, C. Parikh, R. Jain, R. P. Mahto, S. K. Pal, D. C. Chakravarty, Classification and identification of surface defects in friction stir welding: An image processing approach, Journal of Manufacturing Processes 22 (2016) 237–253. doi:10.1016/j.jmapro.2016.03.009

[4] H. Başak, Y. Kayır, E. H. Türkyılmaz, Experimental investigation of the different stirring pin forms caused force and its effects of joining on friction stir welding, El-Cezerî Journal of Science and Engineering 4 (2017) 249–257. (in Turkish) doi:10.31202/ecjse.318209

[5] A. A. Arıcı, A. T. Ertürk, Determination of welded zone properties on friction stir welded polyethylene sheets, Proceedings of 8th International Fracture Conference (2007), pp. 490–497. (in Turkish)

[6] S. Dalkiliç, Friction stir welding and aerospace applications, Journal of Aeronautics & Space Technologies 5 (2012) 25–33. (in Turkish)

[7] J. Mohammadi, Y. Behnamian, A. Mostafaei, H. Izadi, T. Saeid, A. H. Kokabi, A. P. Gerlich, Friction stir welding joint of dissimilar materials between AZ31B magnesium and 6061 aluminum alloys: Microstructure studies and mechanical characterizations. Materials Characterization 101 (2015)189–207. doi:10.1016/j.matchar.2015.01.008

[8] C-H. Ng, S. N. M. Yahaya, A. A. A. Majid, Reviews on aluminum alloy series and its applications, Academia Journal of Scientific Research 5 (2017) 708–716. doi:10.15413/ajsr.2017.0724

[9] R. Kumar, R. Singh, I. P. S. Ahuja, R. Penna, L. Feo, Weldability of thermoplastic materials for friction stir welding – A state of art review and future applications, Composites Part B137 (2018) 1–15. doi:10.1016/j.compositesb.2017.10.039

[10] K. Gangwar, M. Ramulu, Friction stir welding of titanium alloys: A review, Materials and Design 141 (2018) 230–255. doi:10.1016/j.matdes.2017.12.033

[11] R. Çakır, S. Çelik, Effect of welding parameters on microstructure and mechanical properties of friction stir welded Al 5754-Cu, El-Cezerî Journal of Science and Engineering 4 (2017) 82–91. (in Turkish) doi:10.31202/ecjse.289640

[12] Y. Huang, X. Meng, Y. Xie, L. Wan, Z. Lv, J. Cao, J. Feng, Friction stir welding/processing of polymers and polymer matrix composites, Composites: Part A 105 (2018) 235–257. doi:10.1016/j.compositesa.2017.12.005

[13] S. Emami, T. Saeid, R. A. Khosroshahi, Microstructural evolution of friction stir welded SAF 2205 duplex stainless steel, Journal of Alloys and Compounds 739 (2018) 678–689. doi:10.1016/j.jallcom.2017.12.310

[14] G. Ramesh, I. Srimuthunath, N. Santha Kumar, S. Sugandipriya, V. Aravindhan, Characterisation of microstructure and hardness of friction stir welded brass

plate, Materials Today: Proceedings 5 (2018) 2721–2725. doi:10.1016/j.matpr.2018.01.054
[15] A. S. Zoeram, S. H. M. Anijdan, H. R. Jafarian, T. Bhattacharjee, Welding parameters analysis and microstructural evolution of dissimilar joints in Al/bronze processed by friction stir welding and their effect on engineering tensile behaviour, Materials Science & Engineering A 687 (2017) 288–297. doi:10.1016/j.msea.2017.01.071
[16] A. Tongne, C. Desrayaud, M. Jahazi, E. Feulvarch, On material flow in friction stir welded Al alloys, Journal of Materials Processing Technology 239 (2017) 284–296. doi:10.1016/j.jmatprotec.2016.08.030
[17] A. Durdevic, A. Sedmak, A. Zivkovic, D. Durdevic, M. Markovic, M. Milcic, Micro hardness and macrostructures of friction stir welded T-joints, Procedia Structural Integrity 13 (2018) 424–429. doi:10.1016/j.prostr.2018.12.071
[18] S. D. Kumar, S. S. Kumar, Investigation of mechanical behavior of friction stir welded joints of AA6063 with AA5083 aluminum alloys, Mechanics and Mechanical Engineering 23 (2019) 59–63. doi:10.2478/mme-2019-0008
[19] H. M. A. Kumar, V. V. Ramana, M. Pawar, Experimental study on dissimilar friction stir welding of aluminium alloys (5083-H111 and 6082-T6) to investigate the mechanical properties, Materials Science and Engineering 330 (2018) 012076. doi:10.1088/1757-899X/330/1/012076
[19] C. Devanathan, M. Chenthil, D. Prithiviraj, Joining of dissimilar aluminium alloys using friction stir welding, International Journal of Engineering Development and Research 6 (2018) 256–260.
[21] I. Kalemba-Rec, M. Kopyściański, D. Miara, K. Krasnowski, Effect of process parameters on mechanical properties of friction stir welded dissimilar 7075-T651 and 5083-H111 aluminum alloys, The International Journal of Advanced Manufacturing Technology 97 (2018) 2767–2779. doi:10.1007/s00170-018-2147-y
[22] D. Ren, F. Zeng, Y. Liu, L. Liu, Z. He, Friction stir welding of 5754 aluminum alloy with cover sheet, Materials (Basel) 12 (2019) 1765–1775. doi:10.3390/ma12111765
[23] M. M. El Rayes, M. S. Soliman, A. T. Abbas, D. Y. Pimenov, I. N. Erdakov, M. M. Abdel-mawla, Effect of feed rate in FSW on the mechanical and microstructural properties of AA5754 joints, Advances in Materials Science and Engineering 2019 (2019) 4156176. doi:10.1155/2019/4156176
[24] M. M. Z. Ahmed, S. Ataya, M. M. El-Sayed Seleman, A. M. A. Mahdy, N. A. Alsaleh, E. Ahmed, Heat input and mechanical properties investigation of friction stir welded AA5083/AA5754 and AA5083/AA7020, Metals 11 (2021) 068. doi:10.3390/met11010068
[25] M. M. Z. Ahmed, S. Ataya, M. M. El-Sayed Seleman, T. Allam, N. A. Alsaleh, E. Ahmed, Grain structure, crystallographic texture, and hardening behavior of dissimilar friction stir welded AA5083-O and AA5754-H14, Metals 11 (2021) 181. doi:10.3390/met11020181
[26] M. M. Z. Ahmed, M. M. El-Sayed Seleman, Z. A. Zidan, R. M. Ramadan, S. Ataya, N. A. Alsaleh, Microstructure and mechanical properties of dissimilar friction stir welded AA2024-T4/AA7075-T6 T-butt joints, Metals 11 (2021) 128. doi:10.3390/met11010128
[27] B. Ertuğ, L. C. Kumruoğlu, 5083 type Al-Mg and 6082 type Al-Mg-Si alloys for ship building, American Journal of Engineering Research (AJER) 4 (2015) 146–150.
[28] L. A. C. de Filippis, L. M. Serio, D. Palumbo, R. De Finis, U. Galietti, Optimization and characterisation of the friction stir welded sheets of AA 5754-H111: Monitoring of the quality of joints with thermographic techniques, Materials (Basel) 10 (2017) 1165. doi:10.3390/ma10101165
[29] Rajiv S. Mishra, Introduction. in: R. S. Mishra Murray, W. Mahoney (Eds.), Friction Stir Welding and Processing, ASM International, Materials Park, 2007, pp. 1–6. ISBN: 978-0-87170-840-3
[30] J. K. Paik, Mechanical properties of friction stir welded aluminum alloys 5083 and 5383, International Journal of Naval Architecture and Ocean 1 (2009) 39–49. doi:10.2478/IJNAOE-2013-0005
[31] R. Thakur, P. S. Bajwa, Friction stir welding of 5xxx series aluminium alloys: A literature survey, International Research Journal of Engineering and Technology 2 (2016) 1129–1131.
[32] S. Diwahar, K. Anbarasu, P. Deepanchakravarthy, A review on friction stir welding of similar and dissimilar aluminium alloys, International Research Journal of Engineering and Technology 4 (2017) 999–1003.
[33] R. S. Mishra, P. Rani, Friction stir welding of aluminum alloy and the effect of parameters on weld quality – A review, International Journal of Research in Engineering and Innovation 2 (2018) 280–292.
[34] ASTM E8-04, Standard Test Methods for Tension Testing of Metallic Materials West Conshohocken, ASTM International 2020. https://www.astm.org/Standards/E8.htm
[35] F. Tolun, Investigation of the effects of different tool geometries on welded joining of EN AW-5754 and EN AW-5083 aluminum alloys with friction stir welding, Journal of Balıkesir University Institute of Science and Technology 22 (2020) 334–344. (in Turkish) doi:10.25092/baunfbed.680822
[36] A. Şık, Ö. Kayabaş, Examination of mechanical properties of welding zone in aluminium alloy produced by using friction stir welding, Journal of Industrial Arts Education Faculty of Gazi University 11 (2003) 30–43.
[37] A. R. Cisko, J. B. Jordon, D. Z. Avery, T. Liu, L. Brewer, P. G. Allison, R. L. Carino, Y. Hammi, T. W. Rushing, L. Garcia, Experiments and modeling of fatigue behavior of friction stir welded aluminum lithium alloy, Metals 9 (2019) 239. doi:10.3390/met9030293
[38] V. Patel, W. Li, G. Wang, F. Wang, A. Vairis, P. Niu, Friction stir welding of dissimilar aluminum alloy combinations: State-of-the-Art, Metals 9 (2019) 270. doi:10.3390/met9030270
[39] S. Çelik, R. Çakır, Effect of friction stir welding parameters on the mechanical and microstructure properties of the Al-Cu butt joint, Metals 6 (2016) 133. doi:10.3390/met6060133
[40] G. Çam, S. Mistikoğlu, Recent developments in friction stir welding of Al-alloys, Journal of Materials Engineering and Performance 23 (2014) 1936–1953. doi:10.1007/s11665-014-0968-x
[41] M. M. Attallah, C. L. Davis, M. Strangwood, Mi-

crostructure property development in friction stir welds of Al-Mg alloys, Proceedings of 8th International Conference Trends in Welding Research, (2009), pp. 358–363. doi:10.1361/cp2008twr358

[42] D. Li, X. Yang, L. Cui, F. He, X. Zhang, Investigation of stationary shoulder friction stir welding of aluminium alloy 7075-T651, Journal of Materials Processing Technology 222 (2015) 391–398. doi:10.1016/j.jmatprotec.2015.03.036